Molecular Psychiatry (2015) **20,** 1011–1016; doi:10.1038/mp.2014.99;

ORIGINAL ARTICLE

Genomic architecture of human neuroanatomical diversity

R Toro[1,2,3], J-B Poline[4,5], G Huguet[1,2,3], E Loth[6,7], V Frouin[4], T Banaschewski[8], GJ Barker[6], A Bokde[9], C Büchel[10], FM Carvalho[6,7], P Conrod[6,11], M Fauth-Bühler[12], H Flor[13], J Gallinat[14], H Garavan[9,15], P Gowland[15], A Heinz[14], B Ittermann[16], C Lawrence[17], H Lemaître[18,19], K Mann[12], F Nees[13], T Paus[17,20,21], Z Pausova[22], M Rietschel[23], T Robbins[24], MN Smolka[25,26], A Ströhle[14], G Schumann[6,7,27], T Bourgeron[1,2,3,27,28] and the IMAGEN consortium (www.imagen-europe.com)

Human brain anatomy is strikingly diverse and highly inheritable: genetic factors may explain up to 80% of its variability. Prior studies have tried to detect genetic variants with a large effect on neuroanatomical diversity, but those currently identified account for $< 5\%$ of the variance. Here, based on our analyses of neuroimaging and whole-genome genotyping data from 1765 subjects, we show that up to 54% of this heritability is captured by large numbers of single-nucleotide polymorphisms of small-effect spread throughout the genome, especially within genes and close regulatory regions. The genetic bases of neuroanatomical diversity appear to be relatively independent of those of body size (height), but shared with those of verbal intelligence scores. The study of this genomic architecture should help us better understand brain evolution and disease.

Molecular Psychiatry (2015) **20,** 1011–1016; doi:10.1038/mp.2014.99; published online 16 September 2014

INTRODUCTION

Family studies show that a large part of the variability of different human brain structures is determined by genetic factors. Because we know *a priori* the degree of genetic relationship between monozygotic and dizygotic twins, or between members of a family, we can decompose the variability of a phenotype into genetic and environmental components. Various studies have demonstrated in this way that neuroanatomical phenotypes, such as brain volume (BV), cortical surface or white matter microstructure, are highly inheritable, with genetic factors accounting for up to 80% of their variability.[1–4] These results are particularly important for psychiatric research. Different psychiatric disorders have been associated with characteristic changes in brain anatomy, such as a higher incidence of macrocephaly and increased white matter volume in autism,[5] or reduced hippocampal and total BVs in schizophrenia.[6] If these characteristic changes are modulated by the subject's genetic background, then this background may act as a protective factor or as a risk factor for the development of psychiatric conditions. Various efforts have been made to go deeper into the genetics of neuroanatomical diversity through candidate-gene approaches or through agnostic, genome-wide association studies (GWAS).[2,7,8] These approaches have provided important insights on the genetic bases of neuroanatomical diversity; however, for the moment, they account for only a small proportion of the variance.

Here, we used a recently developed method called genome-wide complex trait analysis (GCTA),[9,10] where the combined effect of hundreds of thousands single-nucleotide polymorphisms (SNPs) is considered as a whole—instead of the massive univariate testing approach of classic GWAS. We studied a large cohort of 1765 adolescents from the IMAGEN project,[11] for whom neuroimaging, whole-genome genotyping and behavioural data was collected. As in twin and family studies, we estimated the amount of phenotypic variance explained by genetic relationships among subjects. In contrast, instead of using expected relationships based on pedigree, we used a genome-wide average of the difference in genotyping at each SNP between unrelated subjects. Using different sets of SNPs to compute genetic relationships, we were able to partition neuroanatomical variance into different SNP sets and investigate the genomic architecture of neuroanatomical

diversity at a level of granularity intermediate between that of twin studies and candidate-gene or GWAS. Finally, we simulated phenotypes with different heritabilities and produced by different numbers of causal SNPs to estimate the minimum number of causal SNPs likely to produce our observed results.

MATERIALS AND METHODS

Neuroimaging

Brain scans were obtained from a cohort of 2089 adolescents (14.5 ± 0.4 years old, 51% females) from the IMAGEN project (http://imagen-europe.com) using a standardised 3 T, T1-weighted gradient echo protocol in eight European centres.[11] Scans were first linearly transformed to match the MNI152 atlas using FLIRT from FSL.[12,13] The inverse of the determinant of the transformation matrix was used to estimate the intracranial volume (ICV).[14] Next, the skull was stripped using 3dSkullStrip from AFNI,[15] and the grey matter, white matter and cerebrospinal fluid were automatically segmented using FAST.[16] The skull-stripped versions of the datasets, and the tissue segmentations were visually inspected and manually corrected wherever necessary. Total brain volume (BV) was estimated as the sum of total grey and white matter volumes. Finally, subcortical structures were automatically segmented using FIRST,[17] and their accuracy visually controlled using in-house software. All volumes were $\log_{10}$ converted. Their distribution is illustrated in Supplementary Figure S1. Despite the differences in average volume (from ~1 cm^3 for the amygdala, to ~1300 cm^3 for total BV, Supplementary Figure S1), all structures showed a similar variability – there was a ~1.8-fold change from the smallest to the largest volume in the cohort. The correlation matrix for all phenotypes analysed is shown in Supplementary Table S1.

Genotyping

We used the autosomal SNPs common to the Illumina 610-Quad and Illumina 660W-Quad chips, and strict filtering to conserve high-quality SNPs only (minor-allele frequency >5%, genotyping rate >99%, significance threshold for Hardy–Weinberg equilibrium test $>10^{-6}$, subjects missing genotyping <10%, using PLINK [18]). We further excluded SNPs in strong linkage disequilibrium (R^2>0.9) within a window of 50 SNPs to prevent colinearity in our analyses. The final genotyping data consisted of 269 308 SNPs.

Statistical analyses

We used GCTA to estimate the amount of phenotypic variance captured by genome-wide SNPs. Descriptions of the method can be found in Yang *et al.*,[9] Yang *et al.*,[10] and Lee *et al.*[19] First, we used all SNPs to compute a single genetic relationship matrix (GRM) and we estimated the amount of phenotypic variance captured by this matrix using a mixed-effects linear model. The multiple comparisons were corrected using a global test on the *P*-values of all our phenotypes (Supplementary Methods S1). We used phenotype simulation in GCTA to assess the statistical power of our analyses as well as the minimum number of causal SNPs likely to produce our results (Supplementary Methods S2). The genetic correlation among phenotypes was estimated using the bivariate analysis platform in GCTA. Finally, we partitioned phenotypic variance among different sets of non-overlapping SNPs, and tested *a posteriori* whether any of these partitions captured more variance than what could be expected given its number of SNPs (Supplementary Methods S3). A first partition divided SNPs into genic and non-genic SNPs, based on gene boundaries from the UCSC Genome Browser hg18 assembly. Additional partitions divided SNPs based on their involvement in central nervous system function (Supplementary Methods S4) and minor-allele frequency (Supplementary Methods S5). We also used random partitions of the genome into non-overlapping sets of 20%, 30% and 50% of the SNPs to analyse the correlation between the number of SNPs in a set and the amount of variance captured (Supplementary Methods S6).

Many confounding factors could affect our variance estimates and we used several strategies to control for them. (1) For all our analyses, we included age, sex and scanning centre as covariates. We also analysed the effect of including Pubertal Development Scale[20] scores. Pubertal Development Scale scores did not affect the results and this covariate was no longer included in the model. (2) We excluded subjects with a genetic relationship >0.025 (that is, more related than 3rd or 4th cousins) to prevent an effect of cryptic relatedness (in which case phenotypic similarity could be partly due to shared environment effects or familial causal variants not captured by SNPs). (3) We used Admixture[21] to estimate individual ancestry relative to the reference populations in HapMap 3.[22] The result (Supplementary Figure S2) showed that individuals in our cohort had a strong European-ancestry component. (4) We included the first 10 principal components of the identity-by-state matrix to account for population structure effects.[23] We observed, however, that not including them affected only marginally our variance estimates (0.6% difference, $P=0.93$, two-tailed *t*-test, Supplementary Table S2). (5) We observed that genic SNPs captured more variance than nongenic SNPs (see Results). If our estimates were driven by population structure effects, we could expect an excess of Ancestry Informative Markers (AIMs) within the genic SNP set. We obtained a list of 1442 AIMs from Tian and collaborators,[24] 604 of which were contained among our SNPs. There was no statistically significant difference in the number of AIMs between our genic and nongenic SNP sets (375 genic AIM versus 229 nongenic AIMs, Fisher's exact test $P=0.1723$), and if anything, there was a tendency for AIMs to be underrepresented within the genic SNP set (Fisher's exact test $P=0.089$).

RESULTS

We measured ICV, total BV, as well as the volume of the hippocampus (Hip), thalamus (Th), caudate nucleus (Ca), putamen (Pu), globus pallidus (Pa), amygdala (Amy) and nucleus accumbens (Acc) using validated automatic segmentation programs (Figure 1a). Individuals were whole-genome genotyped, and after various quality control filters, we conserved 269 308 informative, relatively independent ($R^2<0.9$) SNPs in a cohort of 1765 unrelated subjects.

First, we estimated the proportion of the phenotypic variance explained by all SNPs with a linear mixed-effects model with the GRM as the structure of the covariance between subjects using GCTA. We estimated through simulation that we had >50% statistical power to find proportions of phenotypic variance attributable to SNPs (V_G/V_P) values >45%, and >70% statistical power to find V_G/V_P values >55% (Supplementary Figure S3). Using the GCTA Power Calculator,[25] we estimated to have >85% power to detect $V_G/V_P>55\%$, and >70% power to detect $V_G/V_P>45\%$. In all our analyses, we included age, sex and scanning centre as fixed effects. To account for population structure effects, we also included the first 10 principal components of the identity-by-state matrix as covariates. Figure 1b shows the estimated V_G/V_P for the neuroanatomical structures we studied (Supplementary Table S2). The figure includes also estimates of V_G/V_P for height, as well as measurements of verbal intellectual quotient (VIQ) and performance intellectual quotient (PIQ) based on the Wechsler Intelligence Scale for Children. Our estimates for height ($V_G/V_P=56\%$, s.e.=23%, $P=0.0069$), VIQ ($V_G/V_P=56\%$, s.e.=25%, $P=0.013$) and PIQ ($V_G/V_P=52\%$, s.e.=25%, $P=0.02$) were statistically significant, and consistent with those obtained previously in larger populations.[9,26] Because of the smaller size of our population compared with the previous literature, however, the s.e. of our estimations were larger: ~23%. A total of 12 statistical tests were performed. To correct for the multiple comparisons, we used a global test on the *P*-values that evaluated the excess of significant tests (because of the correlation among phenotypes a simple Bonferroni correction would be too conservative). There was a statistically significant ($P=0.0011$) excess of *P*-values <0.05 (see Supplementary Methods S1).

We found that a large proportion of the variance in our neuroanatomical phenotypes was explained by the additive effect of genotyped SNPs. For example, 44% (s.e.=23%, $P=0.031$) of the variance in total BV, 53% (s.e.=23%, $P=0.01$) of the variance in hippocampal volume (Hip) and 54% (s.e.=23%, $P=0.011$) of the variance in ICV. In comparison, the combination of the two largest GWAS to date for BV,[2] Hip[2,7] and ICV[2,8] ($N\sim20\,000$) revealed one SNP associated with hippocampal volume and another associated with ICV, each explaining <0.5% of the variance (this small-effect size is of the same order of magnitude as for genome-wide significant SNPs in other quantitative traits, such as height). Approximately, 50% of the additive genetic factors affecting

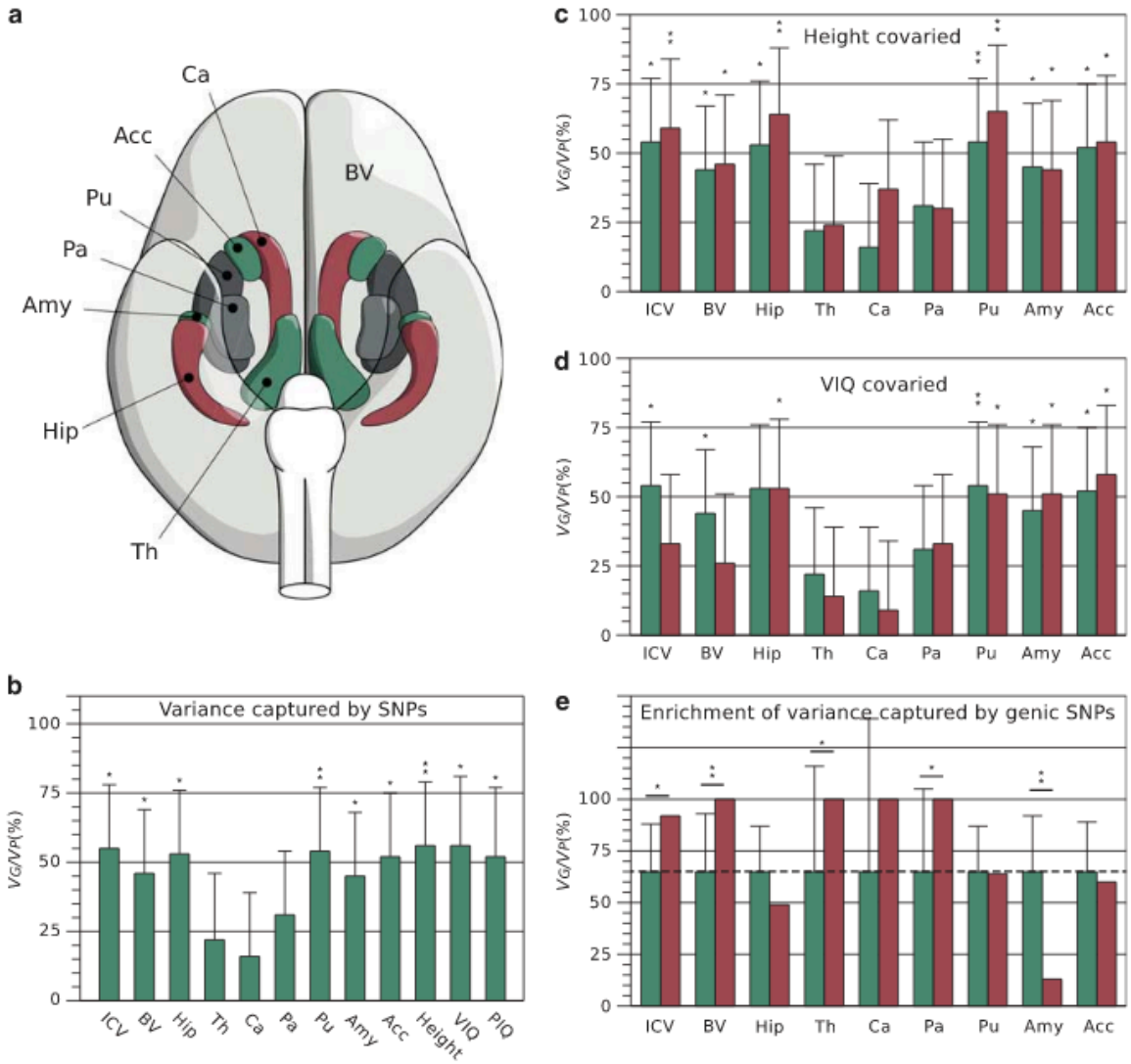

Figure 1. (**a**) Brain phenotypes**.** We measured intracranial volume (not represented), total brain volume (BV, in light grey) and several subcortical structures, Acc, nucleus accumbens; Amy, amygdala; Ca, caudate nucleus; Hip, hippocampus; Pa, pallidum; Pu, putamen and Th, thalamus. (**b**) Variance captured by SNPs. Percentage of phenotypic variance (V_P) due to interindividual genetic relationships (V_G), computed from all genotyped single-nucleotide polymorphisms (SNPs). In addition to brain phenotypes, the bar plot includes estimates of V_G/V_P for height, VIQ and PIQ. (**c**) Effect of covarying body size (height) from brain phenotypes. The proportion of V_G/V_P after covarying height (red bars) did not change substantially compared with those in **b** (green bars), and maintained their statistical significance. (**d**) Effect of covarying VIQ from brain phenotypes. The proportion of V_G/V_P after covarying verbal intellectual quotient (VIQ; red bars) decreased especially for intracranial volume (ICV) and BV, where the estimates were no longer statistically significant (green bars: raw estimates from **b**). (**e**) Enrichment of variance captured by genic SNPs. Genic SNPs (gene boundaries ±50 kbp) represent 64% of all SNPs. If all SNPs explained a similar amount of variance, genic SNPs should explain 64% of the total variance explained by SNPs (dashed line, green bars). They explained significantly more variance than expected for ICV, BV, Th and Pa; significantly less for Amy (red bars, error bars represent test variance). *$P < 0.05$, **$P < 0.01$, uncorrected.

neuroanatomical variability may be then supported by a large number of SNPs, each of small effect.

To get an idea of the minimum number of SNPs likely to produce our results, we used GCTA to simulate 10 000 phenotypes with additive heritability of 50% produced by 1 to 1000 causal SNPs and 10 000 phenotypes produced by 1 to 10 000 causal SNPs. Causal SNPs were randomly selected from among the original 518k genotyped SNPs before R^2 filtering, that is, their effect may be noticeable only through linkage disequilibrium with the ~270k SNPs used to compute the GRM. Their effect sizes were drawn from a normal distribution to obtain 50% heritability. First, we conducted GWAS of all our phenotypes, and recorded the order of magnitude of the smallest *P*-value in each GWAS, which varied from $10^{-5.1}$ to $10^{-6.8}$ (Table 1) . Next, we did the same for each of the 20 000 simulated phenotypes. Figure 2 shows the proportion of simulations with smallest *P*-value of the order of 10^{-5}, 10^{-6} and so on, as a function of the number of causal SNPs used. GWAS of phenotypes produced by very few causal SNPs were more likely to have very small *P*-values. For example, almost all phenotypes produced by <100 causal SNPs had a *P*-value $<10^{-10}$. When the phenotypes were produced by <220 causal SNP, there was at least one *P*-value $<10^{-8}$ in 95% of the cases. In the case of ICV, the smallest *P*-value observed in the GWAS was $10^{-5.95}$. In the simulations, 95% of the GWAS of phenotypes produced by <850 causal SNPs had *P*-values smaller than $10^{-5.95}$. Similarly, the smallest *P*-value in the GWAS of BV was $10^{-6.8}$, and we observed that 95% of the GWAS of phenotypes produced by <420 causal SNPs had *P*-values $<10^{-6.8}$. On the other hand, in

most of the simulations produced by >2000 causal SNPs, the smallest *P*-value was of the order of 10^{-5} or 10^{-6}, like in our data. This suggests that if the distribution of effect sizes of causal SNPs for ICV and BV were similar to that used in our simulations, these phenotypes should likely be produced by at least hundreds of causal SNPs and possibly thousands of them.

Table 1. Order of magnitude of the smallest *P*-value in the GWAS for each phenotype

Phenotype	*−log10(smallest P-value)*
ICV	5.95
BV	6.75
Hip	5.50
Th	5.72
Ca	5.91
Pu	5.49
Pa	5.67
Amy	5.14
Acc	5.60
Height	5.94
VIQ	5.32
PIQ	5.49

Abbreviations: Acc, nucleus accumbens; Amy, amygdala; BV, brain volume; Ca, caudate nucleus; GWAS, genome-wide association studies; Hip, hippocampus; ICV, intracranial volume; Pa, globus pallidus; PIQ, performance intellectual quotient; Pu, putamen; Th, thalamus; VIQ, verbal intellectual quotient.

The variance estimates for different brain structures were heterogeneous, and appeared to be differently related to height, VIQ and PIQ (Supplementary Table S2). For example, although the variance explained by SNPs was high and statistically significant for the Hip ($V_G/V_P = 53\%$, s.e. = 23%, $P = 0.01$), this was not the case for the caudate nucleus ($V_G/V_P = 16\%$, s.e. = 23%, $P = 0.25$)—a structure of comparable volume, geometry and variability that presents a similar correlation with ICV ($r_{Hip/ICV} = 0.51$, $r_{Ca/ICV} = 0.52$) and body size ($r_{Hip/Height} = 0.15$, $r_{Ca/Height} = 0.21$). This shows that the estimates of V_G/V_P were not merely determined by the structure's volume or shape, and could reflect a varying influence of additive genetic and environmental factors. Our variance estimates were not significantly affected by population structure —not including the 10 first principal components of the identity-by-state matrix changed on average the estimates of variance by less than 1% ($P = 0.93$). The estimates of variance did not change significantly either if height or PIQ were covaried (Figure 1c; Supplementary Table S2). In contrast, including VIQ scores as a covariate decreased substantially V_G/V_P estimates for ICV and BV, but not for subcortical structures (Figure 1d). For example, ICV has a moderate correlation with height and VIQ (in our cohort $r_{ICV/Height} = 0.39$ and $r_{ICV/VIQ} = 0.18$). The estimate of V_G/V_P for ICV was not significantly different if height was added as a covariate; however, it decreased from 54 to 32% (no longer statistically significant) if VIQ was included as a covariate. We used the

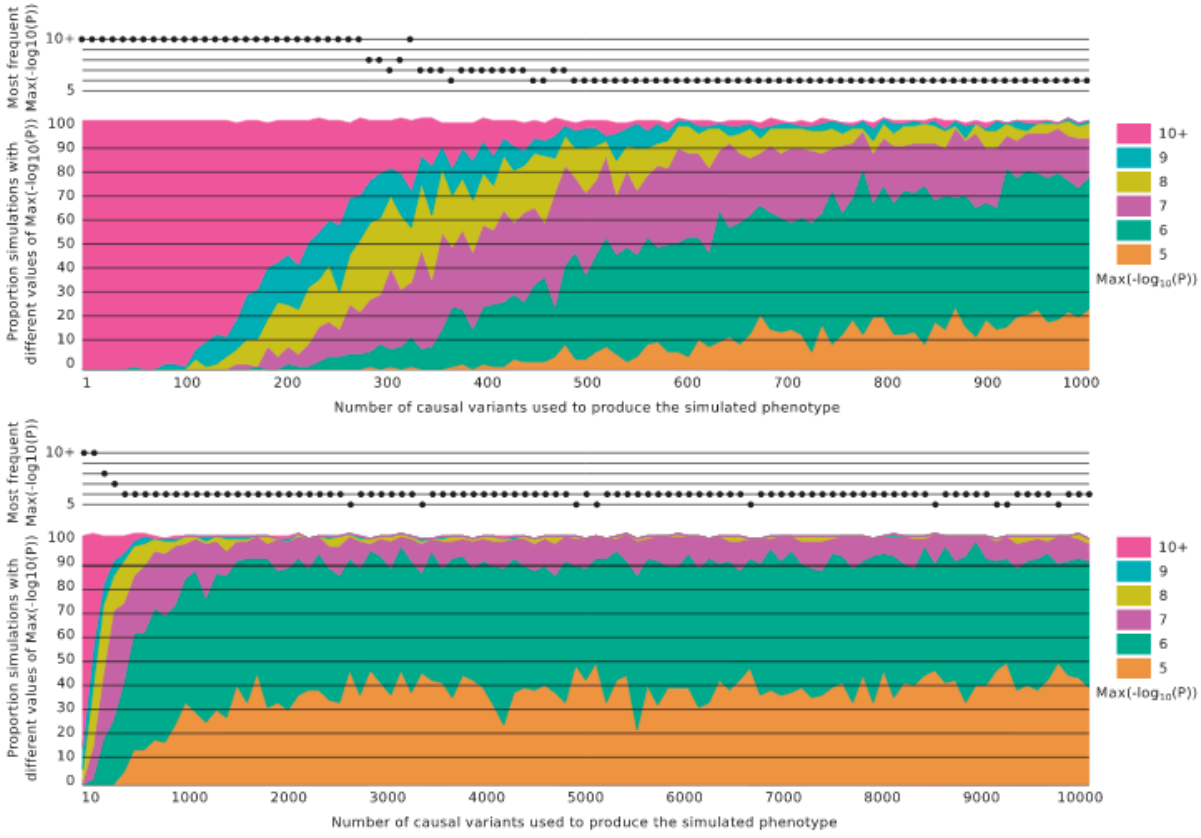

Figure 2. Distribution of smallest *P*-value in the genome-wide association studies (GWAS) with simulated phenotypes as a function of the number of causal single-nucleotide polymorphisms (SNPs) used to generate them. Simulated phenotypes were produced with a number of causal SNPs varying from 1 to 1000 (**a**) and from 1 to 10 000 (**b**). The effect of causal SNPs were drawn from a normal distribution, and the heritability of the simulated phenotypes was fixed at 50%. Ninety five percent of simulated phenotypes with <220 causal SNPs had a smallest *P*-value $< 10^{-8}$. In contrast, simulated phenotypes produced with >500 causal SNPs had most often a smallest *P*-value of the order of 10^{-6} or 10^{-5}. The top plot in **a** and **b** shows the most frequent order of magnitude of the smallest *P*-value as a function of the number of causal SNPs.

bivariate analysis platform in GCTA to estimate the genetic correlation between our phenotypes, that is, the amount of genetic variance shared by each pair of phenotypes (Supplementary Table S3). In particular, these analyses showed indeed a strong genetic correlation between VIQ and ICV ($r_G = 0.95$, $P = 0.0047$), and between VIQ and BV ($r_G = 0.89$, $P = 0.014$), but a small, not statistically significant, genetic correlation between height and ICV ($r_G = 0.20$, $P = 0.25$), and between height and BV ($r_G = 0.23$, $P = 0.24$). Genetic correlation was also weak between PIQ and ICV ($r_G = 0.02$, $P = 0.48$) and between PIQ and BV ($r_G = 0.02$, $P = 0.48$). More than 90% of BV is constituted by the cerebral cortex and its cortico-cortical connections. Our results suggest that the genetic bases of ICV and BV diversity may be shared to a larger extent with those of VIQ than with those of PIQ or body size (height).

A large proportion of the genetic variance captured by SNPs could be due to those located within genes and close regulatory regions. We obtained 20 022 gene boundaries from the UCSC Genome Browser hg18 assembly. We made a first set with all SNPs within these boundaries, and two further sets that included also SNPs 20 kbp and 50 kbp upstream and downstream from the 5′ and 3′ untranslated regions of each gene. Next, we computed GRMs for those three SNP sets (±0, ± 20 and ± 50 kbp genic sets) and their complements. Finally, for each of the three sets, we fitted the same linear mixed-effects model as before (including age, sex, centre and 10 principal components), but using two genetic relationship matrices instead of 1: the genic matrix and its complementary nongenic matrix. Genic SNP sets explained up to 98% of the variance captured by all SNPs (Supplementary Table S4), which was in many cases significantly larger than what could be expected from set length alone (Figure1e; Supplementary Table S5). For ICV, where 54% of the variance can be explained by all genotyped SNPs ($N = 269\,308$), using only SNPs within gene boundaries ($N = 108\,339$) explained 26% of the phenotypic variance (s.e. = 16%, $P = 0.054$), and this proportion increased to 45% (s.e. = 18%, $P = 0.0065$) when the boundaries were expanded to ±20 kbp ($N = 146\,431$), and to 49% (s.e. = 19%, $P = 0.0058$) when the boundaries were expanded to ± 50 kbp ($N = 174\,334$). The genic ± 50 kbp set contained 65% of all genotyped SNPs, but explained 91% of the variance of ICV attributable to SNPs, significantly more than what we would expect from its length alone ($P = 0.014$).

Previous reports have suggested that causal SNPs for height and IQ are relatively homogeneously distributed across the genome, and then, that increasing the number of SNPs used to create a genetic-relationship matrix increases proportionally the amount of phenotypic variance captured.[9] We observed a similar trend in our neuroanatomical phenotypes. We partitioned the genome into non-overlapping sets with different numbers of SNPs, and observed a strong correlation between set length and V_G/V_P ($r = 0.62$ on average). The correlation was the same when only genic SNPs were selected ($r = 0.62$), but smaller, and in most cases not statistically significant when only nongenic SNPs were selected (Supplementary Figure S4).

Finally, we partitioned V_G/V_P based on functional annotation (SNPs within genes involved in central nervous system function[27,28]), and relative minor-allele frequency. We did not observe statistically significant differences in the amount of variance explained by these different SNP sets compared with the expectations based on their length (Supplementary Methods S3; Supplementary Tables S6 and S7).

DISCUSSION

Our analyses indicate that a significant proportion of the heritability of neuroanatomical phenotypes may result from the additive effect of hundreds of small-effect SNPs spread genome-wide. Such SNPs seemed to be largely independent from those related to body size (height) or reflecting population structure in our cohort. They were shared to a greater extent, however, with those associated with VIQ in the case of ICV and BV. An especially important role in determining neuroanatomical diversity appeared to be played by SNPs within genes and close regulatory regions.

Even if many of our variance estimates are large and statistically significant, they are still far from the estimates of heritability in twin studies. Recent twin studies have found that several of the structures we analysed here had heritabilities >80%[29–31] (Supplementary Table S8). This difference may be due in part to a weak linkage disequilibrium between our genotyped SNPs and the real causative variants, to rare alleles with larger effect sizes or to common alleles with even smaller effect sizes.[32,33] Besides, GCTA only captures additive genetic effects, and it has been suggested that part of the difference between heritability estimates in twin studies and GCTA estimates may be due to non-additive genetic factors.[34] It is also possible that the differences may be related to those between the IMAGEN cohort and the cohorts analysed by other studies. For example, the caudate nucleus had the smallest V_G/V_P in our analyses (16%, not significant) but was reported as strongly inheritable by Den Braber *et al.*[31] and Kremen *et al*[29] who studied cohorts of adults (~30 year old and ~55 years old on average, respectively). However, it was reported as having a weaker, not statistically significant heritability by Yoon *et al.*,[30] in a population of 8-year-old children. The lower V_G/V_P of the caudate nucleus in IMAGEN may then reflect an age effect. Furthermore, because of our statistical power, there is a chance of about 15–30% that we may have failed to detect significant V_G/V_P values in our cohort that could have been detected in a larger cohort. Nevertheless, the additive effect of genome-wide SNPs appears as a major determinant of neuroanatomical diversity. Further studies with larger cohorts should be conducted to increase the precision and reliability of our estimations, which should also allow us to detect more subtle differences. For example, we may be able to detect effects related to functional partitions. Finally, our results indicate that cohorts of maybe hundreds of thousands of individuals will be required to make progress in the detection of genes regulating neuroanatomical diversity, which underlines the necessity for international efforts such as the ENIGMA and CHARGE consortia.

Recent studies have highlighted the importance of the additive effect of SNPs in determining anatomical and cognitive diversity in humans, but also their role in psychiatric disorders. In addition to the clear role of rare mutations in the susceptibility to psychiatric disorders,[32,35] genome-wide complex trait analyses have shown that commonly genotyped SNPs capture 23% of the risk to schizophrenia,[28,36] 24% of the risk to Alzheimer's disease[37] and from 17 to 60% of the risk to autism spectrum disorders.[36,38] Due to the small individual effect of these SNPs, GWAS will require very large cohorts to explain any sizeable proportion of the trait's genetic variance.[39] Various structural and functional neuroimaging endophenotypes, on the other hand, have been frequently associated with psychiatric disorders,[40] and using GCTA could inform us about the additive effect of SNPs at a relevant intermediate level, closer to biological processes than cognitive or psychiatric tests. A global view of the genomic architecture of neuroimaging endophenotypes should not only allow us to better understand the biological bases of the susceptibility to psychiatric disorders— helping us, for example, to target future GWAS to more specific chromosomal regions and brain structures—but also to improve our understanding of the biological bases of brain diversity and evolution in humans.

CONFLICT OF INTEREST

The authors declare no conflict of interest.

ACKNOWLEDGMENTS

This work was supported by the European Union-funded FP6 Integrated Project IMAGEN (Reinforcement-related behaviour in normal brain function and psychopathology; LSHM-CT-2007-037286), the FP7 projects ADAMS (Genomic variations underlying common neuropsychiatric diseases and diseases related to cognitive traits in different human populations; 242257), the Innovative Medicine Initiative Project EU-AIMS (115300-2), the Medical Research Council Programme Grant 'Developmental pathways into adolescent substance abuse' (93558), the Swedish Funding Agency FORMAS, the German Bundesministerium und Forschung (FKZ: 01EV0711), Institut Pasteur, CNRS, Université Paris Diderot, the Bettencourt-Schueller Foundation, the Conny-Maeva Foundation, the Orange Foundation, the FondaMental Foundation and the Cognacq-Jay Foundation.

REFERENCES

1 Winkler AM, Kochunov P, Blangero J, Almasy L, Zilles K, Fox PT *et al.* Cortical thickness or grey matter volume? The importance of selecting the phenotype for imaging genetics studies. *NeuroImage* 2010; **53**: 1135–1146.
2 Stein JL, Medland SE, Vasquez AA, Hibar DP, Senstad RE, Winkler AM *et al.* Identification of common variants associated with human hippocampal and intracranial volumes. *Nat Genet* 2012; **44**: 552–561.
3 Blokland GAM, de Zubicaray GI, McMahon KL, Wright MJ. Genetic and Environmental Influences on Neuroimaging Phenotypes: A Meta-Analytical Perspective on Twin Imaging Studies. *Twin Res Hum Genet* 2012; **15**: 351–371.
4 Jahanshad N, Lee AD, Barysheva M, McMahon KL, de Zubicaray GI, Martin NG *et al.* Genetic influences on brain asymmetry: a DTI study of 374 twins and siblings. *NeuroImage* 2010; **52**: 455–469.
5 Amaral DG, Schumann CM, Nordahl CW. Neuroanatomy of autism. *Trends Neurosci* 2008; **31**: 137–145.
6 Steen RG, Mull C, Mcclure R, Hamer RM, Jeffrey A, Steen ANT *et al.* Brain volume in first-episode schizophrenia: Systematic review and meta-analysis of magnetic resonance imaging studies. *Br J Psychiatry* 2012, **188**: 510–518.
7 Bis JC, DeCarli C, Smith AV, van der Lijn F, Crivello F, Fornage M *et al.* Common variants at 12q14 and 12q24 are associated with hippocampal volume. *Nat Genet* 2012; **44**: 545–551.
8 Ikram MA, Fornage M, Smith AV, Seshadri S, Schmidt R, Debette S *et al.* Common variants at 6q22 and 17q21 are associated with intracranial volume. *Nat Genet* 2012; **44**: 539–544.
9 Yang J, Benyamin B, McEvoy BP, Gordon S, Henders AK, Nyholt DR *et al.* Common SNPs explain a large proportion of the heritability for human height. *Nat Genet* 2010; **42**: 565–569.
10 Yang J, Manolio T a, Pasquale LR, Boerwinkle E, Caporaso N, Cunningham JM *et al.* Genome partitioning of genetic variation for complex traits using common SNPs. *Nat Genet* 2011; **43**: 519–525.
11 Schumann G, Loth E, Banaschewski T, Barbot A, Barker G, Büchel C *et al.* The IMAGEN study: reinforcement-related behaviour in normal brain function and psychopathology. *Mol Psychiatry* 2010; **15**: 1128–1139.
12 Jenkinson M, Bannister P, Brady M, Smith S. Improved optimization for the robust and accurate linear registration and motion correction of brain images. *NeuroImage* 2002; **17**: 825–841.
13 Smith SM, Jenkinson M, Woolrich MW, Beckmann CF, Behrens TEJ, Johansen-Berg H *et al.* Advances in functional and structural MR image analysis and implementation as FSL. *NeuroImage* 2004; **23**(Suppl 1): S208–S219.
14 Buckner RL, Head D, Parker J, Fotenos AF, Marcus D, Morris JC *et al.* A unified approach for morphometric and functional data analysis in young, old, and demented adults using automated atlas-based head size normalization: reliability and validation against manual measurement of total intracranial volume. *NeuroImage* 2004; **23**: 724–738.
15 Cox RW. AFNI: software for analysis and visualization of functional magnetic resonance neuroimages. *Comput Biomed Res* 1996; **29**: 162–173.
16 Zhang Y, Brady M, Smith S. Segmentation of brain MR images through a hidden Markov random field model and the expectation-maximization algorithm. *IEEE Trans Med Imaging* 2001; **20**: 45–57.
17 Patenaude B, Smith SM, Kennedy DN, Jenkinson M. A Bayesian model of shape and appearance for subcortical brain segmentation. *NeuroImage* 2011; **56**: 907–922.
18 Purcell S, Neale B, Todd-Brown K, Thomas L, Ferreira MAR, Bender D *et al.* PLINK: a tool set for whole-genome association and population-based linkage analyses. *Am J Hum Genet* 2007; **81**: 559–575.
19 Lee SH, Yang J, Goddard ME, Visscher PM, Wray NR. Estimation of pleiotropy between complex diseases using single-nucleotide polymorphism-derived genomic relationships and restricted maximum likelihood. *Bioinforma Oxf Engl* 2012; **28**: 2540–2542.
20 Carskadon MA, Acebo C. A self-administered rating scale for pubertal development. *J Adolesc Health Off Publ Soc Adolesc Med* 1993; **14**: 190–195.
21 Alexander DH, Novembre J, Lange K. Fast model-based estimation of ancestry in unrelated individuals. *Genome Res* 2009; **19**: 1655–1664.
22 International HapMap Consortium. The International HapMap Project. *Nature* 2003; **426**: 789–796.
23 Price AL, Patterson NJ, Plenge RM, Weinblatt ME, Shadick NA, Reich D. Principal components analysis corrects for stratification in genome-wide association studies. *Nat Genet* 2006; **38**: 904–909.
24 Tian C, Plenge RM, Ransom M, Lee A, Villoslada P, Selmi C *et al.* Analysis and application of European genetic substructure using 300K SNP information. *PLoS Genet* 2008; **4**: e4–e4.
25 Visscher PM, Hemani G, Vinkhuyzen AAE, Chen G-B, Lee SH, Wray NR *et al.* Statistical Power to Detect Genetic (Co)Variance of Complex Traits Using SNP Data in Unrelated Samples. *PLoS Genet* 2014; **10**: e1004269.
26 Davies G, Tenesa A, Payton A, Yang J, Harris SE, Liewald D *et al.* Genome-wide association studies establish that human intelligence is highly heritable and polygenic. *Mol Psychiatry* 2011; **16**: 996–1005.
27 Raychaudhuri S, Korn J, McCarroll S.International Schizophrenia Consortium, Altshuler D, Sklar P. Accurately assessing the risk of schizophrenia conferred by rare copy-number variation affecting genes with brain function. *PLoS Genet* 2010; **6**: e1001097.
28 Lee SH, DeCandia TR, Ripke S, Yang J, Sullivan PF, Goddard ME *et al.* Estimating the proportion of variation in susceptibility to schizophrenia captured by common SNPs. *Nat Genet* 2012; **44**: 247–250.
29 Kremen WS, Prom-Wormley E, Panizzon MS, Eyler LT, Fischl B, Neale MC *et al.* Genetic and environmental influences on the size of specific brain regions in midlife: the VETSA MRI study. *NeuroImage* 2010; **49**: 1213–1223.
30 Yoon U, Perusse D, Lee J-M, Evans AC. Genetic and environmental influences on structural variability of the brain in pediatric twin: deformation based morphometry. *Neurosci Lett* 2011; **493**: 8–13.
31 Den Braber A, Bohlken MM, Brouwer RM, van 't Ent D, Kanai R, Kahn RS *et al.* Heritability of subcortical brain measures: a perspective for future genome-wide association studies. *NeuroImage* 2013; **83**: 98–102.
32 Purcell SM, Moran JL, Fromer M, Ruderfer D, Solovieff N, Roussos P *et al.* A polygenic burden of rare disruptive mutations in schizophrenia. *Nature* 2014; **506**: 185–190.
33 Robinson MR, Wray NR, Visscher PM. Explaining additional genetic variation in complex traits. *Trends Genet* 2014; **30**: 124–132.
34 Trzaskowski M, Dale PS, Plomin R. No genetic influence for childhood behavior problems from DNA analysis. *J Am Acad Child Adolesc Psychiatry* 2013; **52** 1048–1056. e3.
35 Cook EH Jr, Scherer SW. Copy-number variations associated with neuropsychiatric conditions. *Nature* 2008; **455**: 919–923.
36 Cross-Disorder Group of the Psychiatric Genomics Consortium. Genetic relationship between five psychiatric disorders estimated from genome-wide SNPs. *Nat Genet* 2013; **45**: 984–994.
37 Lee SH, Harold D, Nyholt DR, Goddard ME, Zondervan KT, Williams J *et al.* Estimation and partitioning of polygenic variation captured by common SNPs for Alzheimer's disease, multiple sclerosis and endometriosis. *Hum Mol Genet* 2013; **22**: 832–841.
38 Klei L, Sanders SJ, Murtha MT, Hus V, Lowe JK, Willsey AJ *et al.* Common genetic variants, acting additively, are a major source of risk for autism. *Mol Autism* 2012; **3**: 9.
39 Park J-H, Wacholder S, Gail MH, Peters U, Jacobs KB, Chanock SJ *et al.* Estimation of effect size distribution from genome-wide association studies and implications for future discoveries. *Nat Genet* 2010; **42**: 570–575.
40 Meyer-Lindenberg A, Weinberger DR. Intermediate phenotypes and genetic mechanisms of psychiatric disorders. *Nat Rev Neurosci* 2006; **7**: 818–827.